INTERNATIONAL JOURNAL OF CLIMATOLOGY
Int. J. Climatol. (2010)
Published online in Wiley InterScience
(www.interscience.wiley.com) DOI: 10.1002/joc.2125

RMetS
Royal Meteorological Society

Short Communication

Air flow and stability indices in GCM future and control runs

J. A. Hanafin,[a,b,c]* R. McGrath,[b] T. Semmler,[b] S. Wang,[b] P. Lynch,[a] S. Steele-Dunne[a,d] and P. Nolan[a]

[a] *School of Mathematical Sciences, University College Dublin, Belfield, Dublin 4, Ireland*
[b] *Met Éireann, Glasnevin, Dublin 9, Ireland*
[c] *Environmental Change Institute/School of Physics, National University of Ireland, Galway, Ireland*
[d] *Water Resources Section, Faculty Civil Engineering & Geoscience, Delft University of Technology, Postbus 5048, NL-2600 GA Delft, Netherlands*

ABSTRACT: Indices have been used as indicators of synoptic-scale flow strength, shear vorticity, flow direction and static stability over Ireland and Britain. Changes in large-scale dynamic flow and static stability over the European region are expected because of shifting climate patterns, and investigation of how these indices change in future runs of global climate models allows us to estimate how this will affect storm frequency and intensity in the region. Analysis of frequency distributions shows an increase in westerly flows and decreases in most other flow directions, indicating an increase in rainfall for the region. The flow strength on days with strong winds increases in the future runs, as does the number of gale days. The future runs show not only an overall increase in atmospheric stability but also significantly larger areas with stronger instability during periods of extreme instability. Copyright © 2010 Royal Meteorological Society

KEY WORDS regional climate change; climate change modeling; general circulation models; atmospheric stability; Ireland; synoptic scale circulation patterns

Received 31 December 2007; Revised 23 December 2009; Accepted 9 February 2010

1. Introduction

Weather types or circulation patterns have been used extensively to characterize the larger scale atmospheric state into different classes for regional applications, from analysis of trends in these classes to statistical modelling of surface variables based on the classes. An analysis of observed rainfall over Ireland (Sweeney and O'Hare, 1992) found distinct regional patterns of occurrence and intensity of precipitation associated with different Lamb weather types. A number of different approaches have been taken to identify and define the classes, some based on dynamics and some based on statistical analyses. Subjective (Lamb, 1972) and objective (Jones *et al*., 1993; Goodess and Palutikof, 1998; Trigo and DaCamara, 2000) analyses of weather types have been based on mean sea level pressure (MSLP) alone, and also (James, 2007) on MSLP and geopotential height. Singular value decomposition (Santos *et al*., 2007), rotated principal component analyses (PCA) (Kostopoulou and Jones, 2007), empirical orthogonal function (Zorita and von Storch, 1999) and classification and regression tree analyses (Zorita *et al*., 1995) of MSLP have been used. Other approaches to characterizing the atmospheric state prior to downscaling include using self-organizing maps of u and v vectors, humidity and temperature (Hewitson and Crane, 2006) and PCA (Wibig, 1999), correlation map-based classification (Lund, 1963) and fuzzy rule-based classifications (Bardossy *et al*., 2005) of geopotential height.

The aim of this study was to investigate projected changes in weather patterns over Ireland due to climate change, using flow and stability indices determined from re-analysis and global climate model (GCM) fields from 20th century and future runs. The flow indices in question were used in a companion study as predictor fields for a statistical downscaling model of daily precipitation as the indices were shown to be well correlated with rainfall in the region (Hanafin *et al*., 2010). It is of interest to also investigate projected changes in the indices themselves in GCM runs, complementing storm tracking studies (Semmler *et al*., 2008) by examining regional changes in the parameters which provide the conditions for heavy rainfall and severe storms to develop. Changes in the North Atlantic storm track, for example, will influence the frequency and intensity of frontal systems in this particular area and should be apparent from the

* Correspondence to: J. A. Hanafin, Environmental Change Institute/School of Physics, National University of Ireland, Galway, University Road, Ireland. E-mail: Jenny.hanafin@nuigalway.ie

examination of the flow strength and direction over the region.

The air flow indices used in this study as indicators of the synoptic situation were the vorticity, direction and strength of flow, calculated from MSLP fields following the objective scheme of Jones *et al*. (1993). Atmospheric stability indices, while well correlated with severe storm activity (Schultz, 1989), and used in climatological studies of recent weather (DeRubertis, 2006), are not often used in the analysis of GCM output. One such index was investigated here, the Showalter index (SI) that is used by weather forecasters for thunderstorm potential. For thunderstorms to develop, there must be conditional instability, a sufficiently deep moist layer in the lower troposphere and uplift to initiate the convection. The SI is calculated by lifting an air parcel dry-adiabatically from 850 hPa to the lifting condensation level and then moist-adiabatically to 500 hPa. The index is the difference between the final temperature of the air parcel and its environment, and it is used by forecasters to estimate the likelihood of thunderstorm development. As the SI becomes more negative, it indicates increasingly unstable conditions, which are a prerequisite for convective development. The SI scored very highly compared with similar indices for its ability to forecast thunderstorm *versus* non-thunderstorm days, severe *versus* non-severe thunderstorms and the likelihood of hail, using a Heidke skill score (Kunz, 2007).

Descriptions of the re-analysis and GCM used in this work, along with the definition and description of the flow and stability indices used are given in the following section. A comparison of the frequency and intensity of the indices calculated from the GCM control run with those calculated from the ERA-40 re-analysis fields is then outlined. This is followed by a comparison of the indices calculated from the control and future GCM runs and a discussion of the results.

2. Data and methods

The ERA-40 re-analysis (Uppala *et al*., 2005) was used here to evaluate how well the GCMs can reproduce the current climate. This re-analysis is produced using a consistent T159 spectral model with 60 vertical levels and a three-dimensional variational data assimilation process over the period used here from 1961 to 2000. A number of intercomparisons between the ERA-40 re-analysis and that produced by the National Center for Environmental Protection/National Consortium for Atmospheric Research (NCEP/NCAR) have been carried out, some of which focus entirely on storm tracking applications (Trigo, 2006; Wang *et al*., 2006; Raible *et al*., 2008). As there is no study available which definitively recommends one over the other, however, the ERA-40 re-analysis was used here due to the higher resolution fields available ($1.125^\circ \times 1.125^\circ$ compared to $2.5^\circ \times 2.5^\circ$ for NCEP/NCAR).

The GCM used was European Centre Hamburg (ECHAM)5, in the configuration used for the IPCC Fourth Assessment Report (IPCC, 2007) experiments. This model was developed at the Max Planck Institute (MPI), Germany and has 31 vertical levels, a horizontal resolution of $1.9^\circ \times 1.9^\circ$ (Roeckner *et al*., 2003) and is coupled to the MPI ocean model with a $1.5^\circ \times 1.5^\circ$ horizontal resolution and 40 vertical levels (Marsland *et al*., 2003). An evaluation of the models used in the Intergovernmental Panel for Climate Change (IPCC) FAR (van Ulden and van Oldenborgh, 2006) found that the ECHAM5 model was one of the better performing models for both global and European MSLP fields when compared with the ERA-40 re-analysis. For this study, air flow indices were calculated from daily MSLP fields over the region 40 to 65°N and 30 °W to 15 °E and stability indices were calculated from the available 500 hPa temperature, 500 hPa relative humidity and 850 hPa temperature fields over the control run. This is referred to as the 20C run, in which the model is run with observed 20th century emissions until 2000 and then with concentrations fixed until 2100 to determine the level of committed climate change. The control period was from 1961 to 2000 and the domain used for both ERA-40 and ECHAM5 was 45 to 65°N and 20 °W to 15 °E.

The IPCC has defined standard greenhouse gas emission scenarios for use in the examination of projected climate changes based on various socioeconomic, technological and energy use factors. Two scenarios were used for the projections presented here, the SRA1B and the SRA2. The SRA1B scenario describes a world in which emissions are relatively high until the 2050 s and then begin to decrease, so that greenhouse gas (GHG) emissions in 2100 are only slightly higher than the 2020 levels. In the SRA2 scenario, emissions continue to rise until 2100. The future period was from 2061 to 2100.

The air flow indices were determined using the method described by Jones *et al*. (1993). A shear vorticity index (V), a flow strength index (F) and a flow direction index (D) were determined from the MSLP field of the ERA40 re-analysis and that of the ECHAM5 output for different scenarios. These are synoptic-scale indices, calculated from the MSLP field from 45 to 65°N and 20 °W to 10 °E so centred over Ireland and Britain, and including a portion of the north-eastern Atlantic and the north-western European continent. The indices are calculated using finite differences of the MSLP field between a set of grid points, the reader is referred to Jones *et al*. (1993) for complete details. The flow strength index has units of hPa per 10° latitude at 55°N, which is equivalent to 2.2 km/h. The shear vorticity index also has units of hPa per 10° latitude at 55°N, and is simply an indicator of cyclonic ($Z > 0$) or anti-cyclonic ($Z < 0$) flow over the region. Additionally, a gale index (G) was calculated from the vorticity and flow strength indices, where $G = (V^2 + (0.5F)^2)^{1/2}$ and gale days were defined as days when $G > 30$. This index was developed as an objective definition of the frequency of occurrence of gale force winds and calibrated using 10 years of observations of monthly gale frequencies in this region (Jenkinson and Collins, 1977).

Table I. SI category thresholds.

SI	Category	Stability
$-2 < \text{SI} < 1$	1	Marginal instability
$-3 < \text{SI} < -2$	2	Moderate instability
$-6 < \text{SI} < -3$	3	Large instability
$\text{SI} < -6$	4	Extreme instability

The SI thresholds used in the different categories are given in Table I, with an indication of how stable each category is. The SI was calculated for the daily mean temperature and humidity fields from ERA-40 and ECHAM5 20C from 1961 to 2000 and from the ECHAM5 A1B and A2 scenario runs for 2061–2100 over the domain. This index is well correlated with severe storms (DeRubertis, 2006; Kunz, 2007), and was found to be the best indicator of pre-convective activity at different latitudes (Sanchez *et al*., 2009). A less stable atmosphere will increase the probability of more frequent and more intense storms occurring in the future. It is not, however, a perfect indicator of significant convective activity: it does not perform well when a dry layer is present at 850 hPa; and while it is a necessary condition for thunderstorm development, some source of uplift is also required. The latter requirement poses difficulties for most atmospheric stability indices. Using daily mean fields will result in an underestimate of the frequency of systems passing through the region compared to an analysis of 6- or 12-hourly values. However, the same analysis is applied to the re-analysis and to the GCM data, so the comparison of current with future climate scenarios is consistent within the study, the aim of which was to estimate how regional atmospheric stability changes within the climate model.

3. Results

3.1. Comparison of ECHAM-5 and ERA-40

3.1.1. Air flow indices

While studies have shown that ECHAM5 is one of the better GCMs at reproducing MSLP fields, how the GCM reproduces the frequency distribution of the air flow indices is of interest here. Figure 1 shows the frequency distribution of synoptic-scale (a) flow direction, (b) vorticity and (c) flow strength calculated from ERA40 and 20C ECHAM5 MSLP fields. While the comparison is good in general, the GCM has more instances of southerly/southwesterly flow and fewer of easterly/northeasterly. Table II shows that the differences for flow direction bins of 45° are less than 1%, apart from the southwesterly flows. The GCM tends also towards more positive vorticity (cyclonic flows) and higher flow strengths.

A similar analysis was carried out for each season. December–January–February and September–October–November (not shown) flow direction and strength compare extremely well for the two datasets, with better

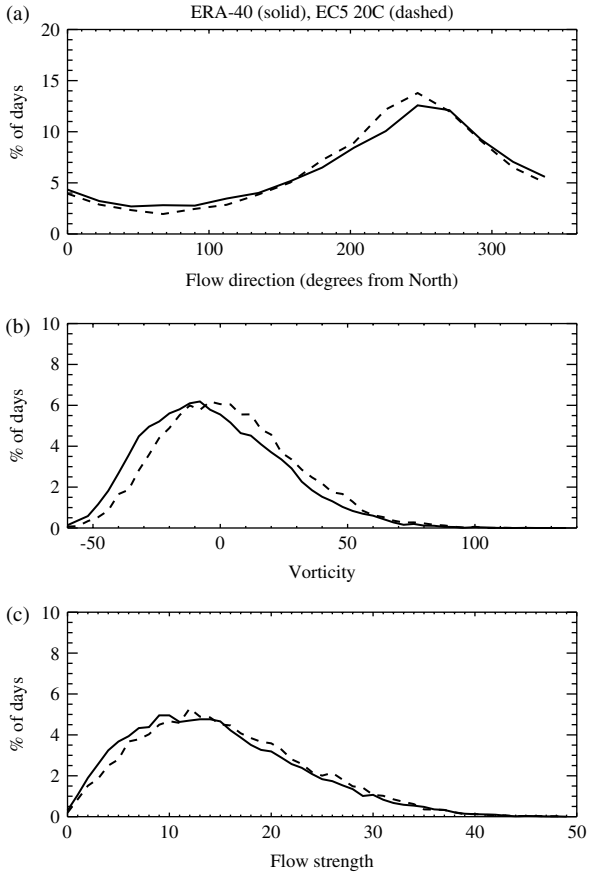

Figure 1. Frequency distribution of air flow indices: (a) direction, (b) vorticity and (c) strength, calculated from ERA-40 (solid line) and ECHAM-5 20C run over the control period (1961–2000).

Table II. Frequency of occurrence of days with flow direction in the bins used in this study for ERA-40 and ECHAM-5.

Flow direction (degrees from North)	Flow direction	Percentage occurrence, 1961–2000	
		ERA-40	EC5-20C
67.5–112.5	E	5.82	4.82
337.5–360; 0–22.5	N	8.62	7.74
22.5–67.5	NE	5.59	4.72
292.5–337.5	NW	14.11	13.54
157.5–202.5	S	13.24	14.21
112.5–157.5	SE	8.30	7.55
202.5–247.5	SW	20.60	23.83
247.5–292.5	W	23.73	23.60

See also Figure 1(a).

than 1% agreement for most bins. The largest differences in flow direction frequencies are in June–July–August (Figure 2), where the ECHAM5 overestimates southerly to southwesterly flows by 4–5% and consistently underestimates flow directions <200°. Vorticity tends to be more cyclonic for all seasons in ECHAM5.

3.1.2. Stability index

To investigate how atmospheric stability may change in the future, a number of metrics were used. The

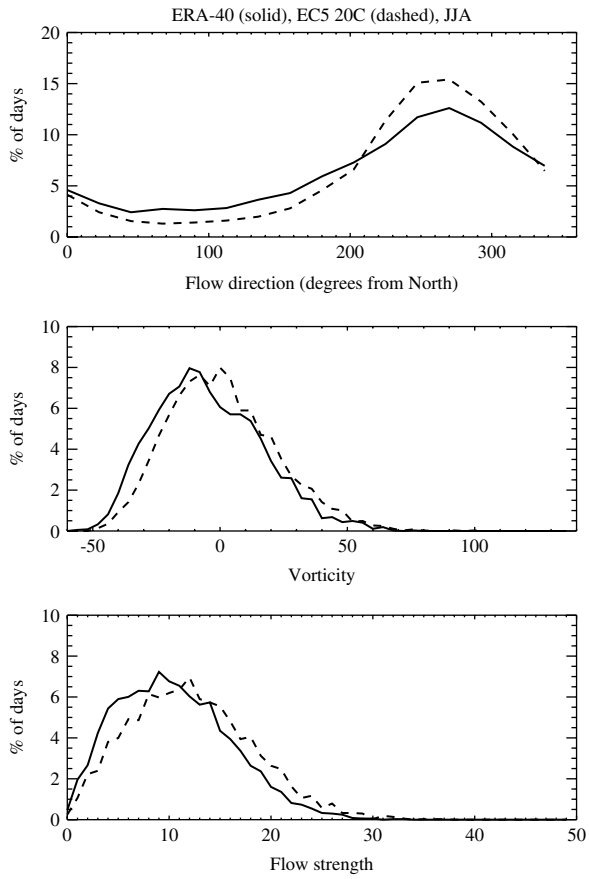

Figure 2. As Figure 1, for June–August only.

20C ECHAM5 run was compared with the ERA-40 to evaluate how well the GCM can reproduce the SI. First, the mean SI was calculated over all gridpoints (Figure 3(a)) and then over all gridpoints falling into category 4, which represents the extremely unstable cases (Figure 3(b)). The GCM underestimates the stability index on average, i.e. predicts less stable conditions than ERA-40. It does a very good job of reproducing the extreme instability values, however, as shown in Figure 3(b). There are only 3 years which have no values in category 4 for ERA-40, but 12 for ECHAM5 in this 40-year period, so while the model reproduces the values, it underestimates the frequency of these events.

To evaluate the spatial extent and frequency of occurrence of stable and unstable gridpoints, two further metrics were investigated and shown in Figure 4. The mean percentage coverage is the mean percentage of all gridpoints which fall into categories 1–4, calculated over the days on which there is at least one gridpoint in the category. This gives an indication of the spatial extent of stable and potentially unstable regions, unaffected by any frequency biases. Figure 4(b) shows the number of days per year when at least one gridpoint in the region fell into each category, giving an indication of how frequently unstable conditions occur. The GCM underestimates both the spatial extent and the frequency of unstable conditions (categories 2–4).

3.2. Comparison of ECHAM-5 scenario runs and control run

3.2.1. Air flow indices

When comparing the frequency distributions of the A1B and A2 scenarios with the 20C ECHAM5 run (Figure 5), some trends are apparent. First, the frequency of northerly, easterly and southerly flows is reduced in the future runs, whereas that of southwesterly and westerly flows has increased. The vorticity index shows an increase in anti-cyclonic flows at the expense of cyclonic flows. Flow strength is reduced slightly for the weaker flows but it is increased for the stronger flows. Seasonal analysis shows similar changes for all seasons, except for June–July–August vorticity, which shows a significant trend towards higher values, both positive and negative.

3.2.2. Stability index

Figures 6 and 7 show the same metrics as Figures 3 and 4, but now for the 2061–2100 period under the A1B and A2 scenarios. The mean SI falls within that of the ERA-40 and the ECHAM5 20C mean (upper and lower lines in Figure3(a), respectively), showing that atmospheric stability has increased in the future runs compared to the control run. The mean extreme values are larger for both of these runs, however, with more variability and more frequent large negative (<-7) values. Figure 7 shows that both the spatial extent and frequency of the unstable categories 2–4 which were underestimated in the 20C run, increase in the scenario runs and are comparable to the ERA-40 control values.

Table III shows the increase in the 40-year mean values from the 20C run to the scenario runs. While the mean SI shows an increase of only 6–8%, the mean category 4 SI shows increases of 52–54%. The spatial extent of large instability category 3 has increased by 109–138%, and that of category 4 has increased by 233–357%. The frequencies have increased by 62–78% for category 3 and 146–274% for category 4. These results indicate that extremely unstable atmospheric conditions are likely to occur more often, have larger spatial extent and be more unstable than that in the current climate, even though the overall stability has increased.

4. Summary and discussion

Changes in prevailing air flows may be one result of changes in the temperature gradient between the equator and the poles due to global warming. A study of the frequency and intensity of storm tracks in the northern and southern hemisphere in ECHAM5 A1B scenario compared to the 20C run found a reduction in the number of extratropical storms in winter by 4–6% in both hemispheres, with a decrease of 3% in the more intense storms (Bengtsson *et al.*, 2006). The storm tracks were found to move poleward in both hemispheres, however, resulting in an increase in both the frequency

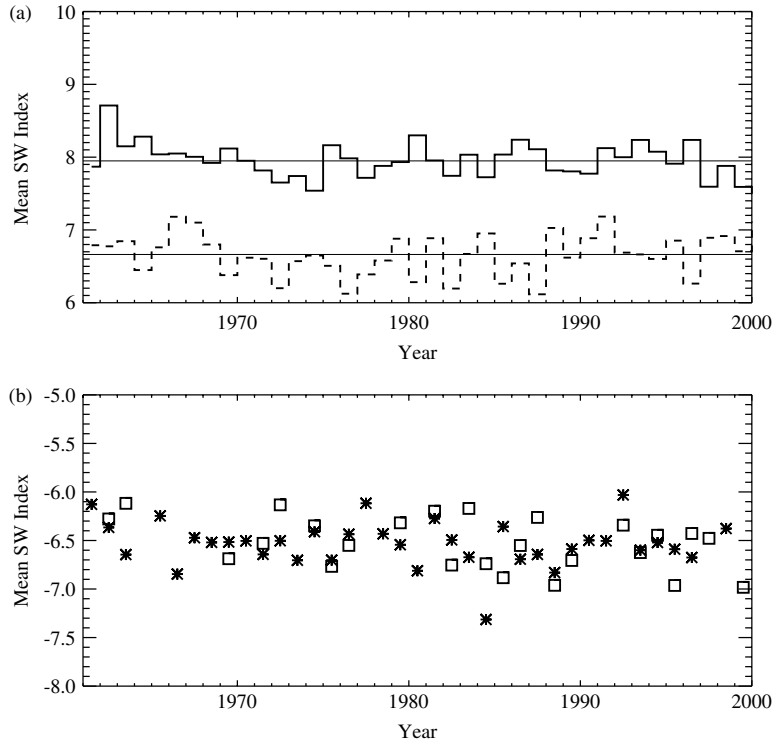

Figure 3. (a) Mean SI for ERA-40 (solid) and ECHAM-5 20C (dashed) control run for all gridpoints. (b) Mean SI for category 4 gridpoints from ECHAM-5 (boxes) and ERA-40 (asterisks).

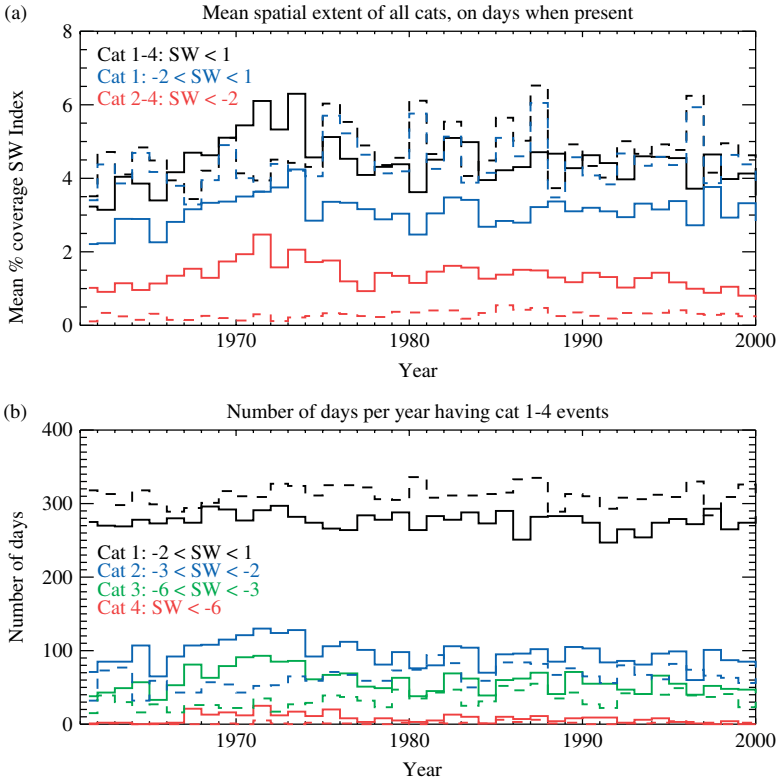

Figure 4. (a) Percentage of all gridpoints falling into SI categories 1–4, category 1 and categories 2–3; (b) mean number of days per year having any gridpoint in categories 1–4 for ERA-40 (solid) and ECHAM-5 20C run (dashed).

and intensity of storms over Ireland and Britain and to the north and west for most of the year and a decrease in the Mediterranean. A larger poleward shift occurs in the summer, bringing the storm track over the Atlantic to the northwest of Ireland. Again, although hemispheric differences in storm intensity were small, the northeast

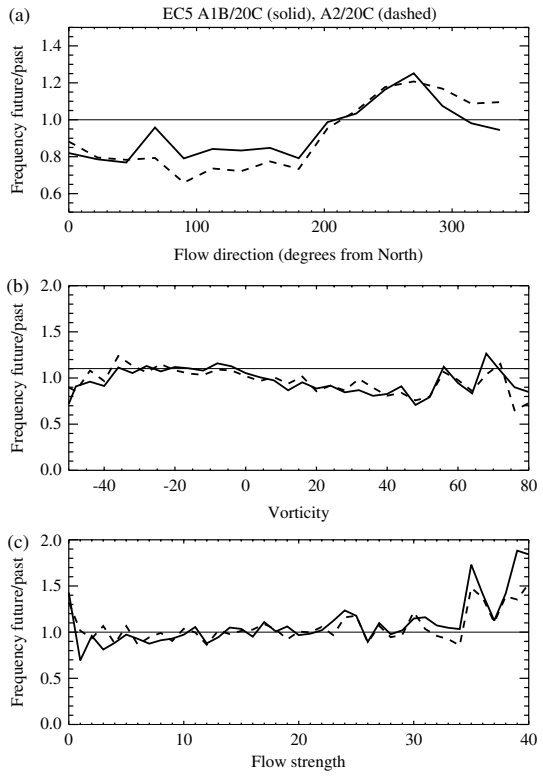

Figure 5. Ratio of the frequency distribution of air flow indices: (a) direction, (b) vorticity and (c) strength, of the A1B (solid) and A2 (dashed) scenarios to the 20C control run.

Atlantic region showed a marked increase in the more intense storms in the 21C.

This study used air indices to investigate expected trends in synoptic flows and atmospheric stability over northwest Europe. Calculation of these indices is straightforward and requires a very limited number of GCM fields, so they are ideal for multi-model ensemble applications. Previous studies have found good correlation between these indices and surface conditions in this region, particularly with respect to rainfall (Jenkinson and Collins, 1977; Sweeney and O'Hare, 1992; Conway *et al*., 1996; Turnpenny *et al*., 2002).

It has been shown here that the frequency of westerly flows is projected to increase in future runs of the ECHAM5 model. For Ireland, these flows are associated with precipitation from the moist airmasses coming over the Atlantic. The frequency of drier easterly flows decreases in the future runs. The frequency of stronger air flow increases, so the probability of strong winds which are capable of causing damage increases. This is evident from increases in the number of gale days, the number of days with strong flow and the mean flow strength on days with strong flow (Table IV).

The SI is a measure of the local static stability, very useful for determining areas of extreme instability necessary for thunderstorm development. The GCM used in this study projects that the atmosphere will become more stable in the future, but extreme values will become more frequent. Both the spatial extent and the magnitude of extreme instabilities increase dramatically between control and future GCM runs in this analysis.

Acknowledgements

This work was carried out under the Community Climate Change Consortium for Ireland (C4I) Project,

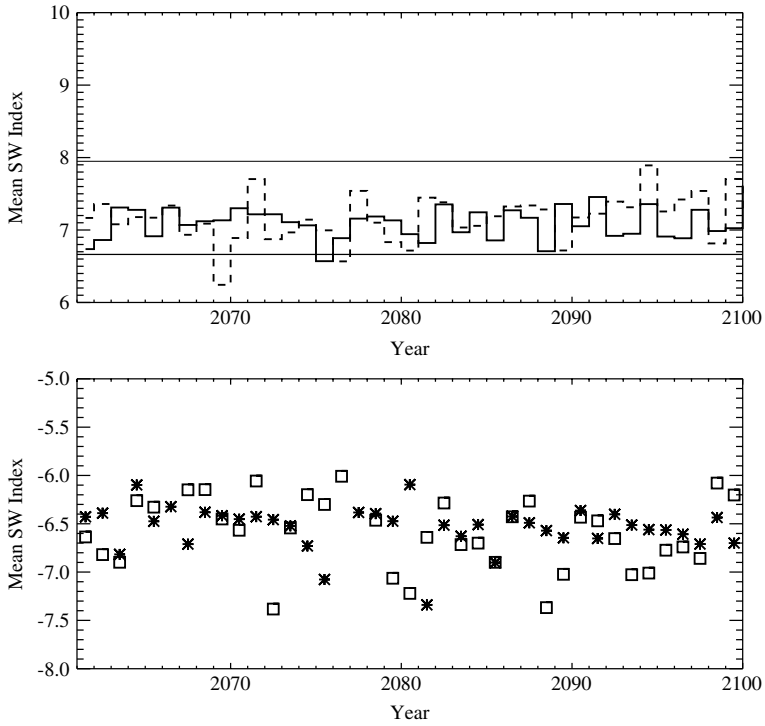

Figure 6. As Figure 3, but for ECHAM-5 A1B (solid, boxes) and A2 (dashed, asterisks) scenarios.

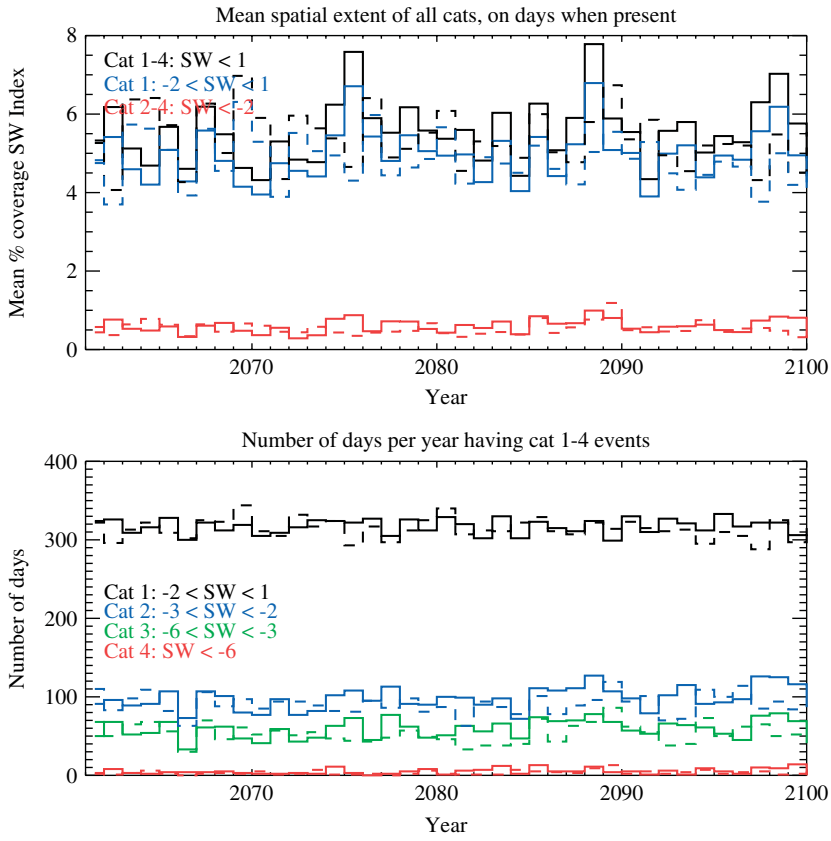

Figure 7. As Figure 4, but for ECHAM-5 A1B (solid) and A2 (dashed) scenarios.

Table III. Changes in spatial extent and frequency of gridpoints in SI categories.

	Mean SI	Area (%)				Frequency (number of days)				Mean category 4
		Category 1	Category 2	Category 3	Category 4	Category 1	Category 2	Category 3	Category 4	
A1B/20C	1.06	1.12	1.86	2.38	4.57	1.02	1.53	1.78	3.74	1.52
A2/20C	1.08	1.10	1.73	2.09	3.33	1.01	1.41	1.62	2.46	1.54

Table IV. Values of some of the metrics used to estimate changes in air flow indices.

Model	Number of gale days ($G > 30$)	Number of cyclonic days ($Z > 0$)	Number of strong flow days ($F > 30$)	Mean flow strength on strong flow days
era40	1784	6653	832	34.32
ec5_20C_1961_2000	2074	8097	897	34.14
ec5_A1B_2061_2100	2209	7502	1080	34.46
ec5_A2_2061_2100	2100	7583	1021	34.61

funded by the Irish Environmental Protection Agency, Met Éireann, Sustainable Energy Ireland and the Irish Higher Education Authority. The work was also supported by the CosmoGrid project, funded under the Programme for Research in Third Level Institutions (PRTLI) administered by the Irish Higher Education Authority. We thank the model and data group at Max Planck Institute for Meteorology in Hamburg, Germany for the ECHAM5-OM1 data.

References

Bardossy A, Bogardi I, Matyasovszky I. 2005. Fuzzy rule-based downscaling of precipitation. *Theoretical and Applied Climatology* **82**(1–2): 119–129.

Bengtsson L, Hodges KI, Roeckner E. 2006. Storm tracks and climate change. *Journal of Climate* **19**(15): 3518–3543.

Conway D, Wilby RL, Jones PD. 1996. Precipitation and air flow indices over the British Isles. *Climate Research* **7**(2): 169–183.

DeRubertis D. 2006. Recent trends in four common stability indices derived from US radiosonde observations. *Journal of Climate* **19**(3): 309–323.

Goodess CM, Palutikof JP. 1998. Development of daily rainfall scenarios for southeast Spain using a circulation-type approach to downscaling. *International Journal of Climatology* **18**(10): 1051–1083.

Hanafin JA, Semmler T, McGrath R, Lynch P, Wang S, Steele-Dunne S, Nolan P. 2010. Statistical downscaling of precipitation over Ireland from a GCM using air flow indices. *Journal of Hydrology*. (submitted).

Hewitson BC, Crane RG. 2006. Consensus between GCM climate change projections with empirical downscaling: Precipitation downscaling over South Africa. *International Journal of Climatology* **26**(10): 1315–1337.

IPCC. 2007. *Climate Change 2007: The Physical Science Basis. Contribution of Working Group I to the Fourth Assessment Report of the Intergovernmental Panel on Climate Change*. Cambridge University Press: Cambridge, United Kingdom and New York, NY, USA.

James PM. 2007. An objective classification method for Hess and Brezowsky Grosswetterlagen over Europe. *Theoretical and Applied Climatology* **88**(1–2): 17–42.

Jenkinson AF, Collins FP. 1977. *An Initial Climatology of Gales Over the North Sea*. Meteorological Office: Bracknell.

Jones PD, Hulme M, Briffa KR. 1993. A comparison of lamb circulation types with an objective classification scheme. *International Journal of Climatology* **13**(6): 655–663.

Kostopoulou E, Jones PD. 2007. Comprehensive analysis of the climate variability in the eastern Mediterranean. Part I: map-pattern classification. *International Journal of Climatology* **27**(9): 1189–1214.

Kunz M. 2007. The skill of convective parameters and indices to predict isolated and severe thunderstorms. *Natural Hazards and Earth System Sciences* **7**(2): 327–342.

Lamb HH. 1972. *British Isles Weather Types and a Register of the Daily Sequence of Circulation Patterns*. Meteorological Office, HMSO: London.

Lund IA. 1963. Map-pattern classification by statistical methods. *Journal of Applied Meteorology* **2**: 56–65.

Marsland SJ, Haak H, Jungclaus JH, Latif M, Roske F. 2003. The Max-Planck-Institute global ocean/sea ice model with orthogonal curvilinear coordinates. *Ocean Modelling* **5**(2): 91–127.

Raible CC, Della-Marta PM, Schwierz C, Wernli H, Blender R. 2008. Northern hemisphere extratropical cyclones: a comparison of detection and tracking methods and different reanalyses. *Monthly Weather Review* **136**(3): 880–897.

Roeckner E, Bäuml G, Bonaventura L, Brokopf R, Esch M, Giorgetta M, Hagemann S, Kirchner I, Kornblueh L, Manzini E, Rhodin A, Schlese U, Schulzweida U, Tompkins A. 2003. *The Atmospheric General Circulation Model ECHAM5. Part 1: Model Description*. Max Planck Institute for Meteorology: Hamburg, Germany.

Sanchez JL, Marcos JL, Dessens J, Lopez L, Bustos C, Garcia-Ortega E. 2009. *Atmospheric Research* **93**(1–3): 446–456.

Santos JA, Corte-Real J, Ulbrich U, Palutikof J. 2007. European winter precipitation extremes and large-scale circulation: a coupled model and its scenarios. *Theoretical and Applied Climatology* **87**(1–4): 85–102.

Semmler T, Varghese S, McGrath R, Nolan P, Wang S, Lynch P, O'Dowd C. 2008. Relationship of several stability indices to convective weather events in northeast Colorado. *Weather Forecasting* **4**: 73–80.

Semmler T, *et al*. 2008. Regional climate model simulations of North Atlantic cyclones: frequency and intensity changes. *Climate Research* **36**(1): 1–16.

Sweeney JC, O'Hare GP. 1992. Geographical variations in precipitation yields and circulation types in Britain and Ireland. *Transactions of the Institute of British Geographers* **17**(4): 448–463.

Trigo IF. 2006. Climatology and interannual variability of storm-tracks in the Euro-Atlantic sector: a comparison between ERA-40 and NCEP/NCAR reanalyses. *Climate Dynamics* **26**(2–3): 127–143.

Trigo RM, DaCamara CC. 2000. Circulation weather types and their influence on the precipitation regime in Portugal. *International Journal of Climatology* **20**(13): 1559–1581.

Turnpenny JR, Crossley JF, Hulme M, Osborn TJ. 2002. Air flow influences on local climate: comparison of a regional climate model with observations over the United Kingdom. *Climate Research* **20**(3): 189–202.

Uppala SM, Kallberg PW, Simmons AJ, Andrae U, Bechtold VD, Fiorino M, Gibson JK, Haseler J, Hernandez A, Kelly GA, Li X, Onogi K, Saarinen S, Sokka N, Allan RP, Andersson E, Arpe K, Balmaseda MA, Beljaars ACM, Van De Berg L, Bidlot J, Bormann N, Caires S, Chevallier F, Dethof A, Dragosavac M, Fisher M, Fuentes M, Hagemann S, Holm E, Hoskins BJ, Isaksen L, Janssen PAEM, Jenne R, McNally A, Mahfouf JF, Morcrette JJ, Rayner NA, Saunders RW, Simon P, Sterl A, Trenberth KE, Untch A, Vasiljevic D, Viterbo P, Woollen J. 2005. The ERA-40 re-analysis. *Quarterly Journal of the Royal Meteorological Society* **131**(612): 2961–3012.

van Ulden AP, van Oldenborgh GJ. 2006. Large-scale atmospheric circulation biases and changes in global climate model simulations and their importance for climate change in Central Europe. *Atmospheric Chemistry and Physics* **6**: 863–881.

Wang XLL, Swail VR, Zwiers FW. 2006. Climatology and changes of extratropical cyclone activity: comparison of ERA-40 with NCEP-NCAR reanalysis for 1958–2001. *Journal of Climate* **19**(13): 3145–3166.

Wibig J. 1999. Precipitation in Europe in relation to circulation patterns at the 500 hPa level. *International Journal of Climatology* **19**(3): 253–269.

Zorita E, Hughes JP, Lettemaier DP, Vonstorch H. 1995. Stochastic characterization of regional circulation patterns for climate model diagnosis and estimation of local precipitation. *Journal of Climate* **8**(5): 1023–1042.

Zorita E, von Storch H. 1999. The analog method as a simple statistical downscaling technique: comparison with more complicated methods. *Journal of Climate* **12**(8): 2474–2489.

